Author(s): Altowyan, Mezna Saleh; Soliman, Saied M.; Haukka, Matti; Al-Shaalan, Nora H.; Alkharboush, Aminah A.; Barakat, Assem

Title: Synthesis of Unexpected Dimethyl 2-(4-Chlorophenyl)-2,3-dihydropyrrolo[2,1-a]isoquinoline-1,3-dicarboxylate via Hydrolysis/Cycloaddition/Elimination Cascades : Single Crystal X-ray and Chemical Structure Insights

Year: 2022

Version: Published version

crystals

MDPI

Article

Synthesis of Unexpected Dimethyl 2-(4-Chlorophenyl)-2,3-dihydropyrrolo[2,1-*a*]isoquinoline-1,3-dicarboxylate via Hydrolysis/Cycloaddition/Elimination Cascades: Single Crystal X-ray and Chemical Structure Insights

Mezna Saleh Altowyan [1], Saied M. Soliman [2], Matti Haukka [3], Nora H. Al-Shaalan [1], Aminah A. Alkharboush [1] and Assem Barakat [4,*]

[1] Department of Chemistry, College of Science, Princess Nourah Bint Abdulrahman University, P.O. Box 84428, Riyadh 11671, Saudi Arabia; msaltowyan@pnu.edu.sa (M.S.A.); nhalshaalan@pnu.edu.sa (N.H.A.-S.); Amina84w@gmail.com (A.A.A.)
[2] Department of Chemistry, Faculty of Science, Alexandria University, P.O. Box 426, Ibrahimia, Alexandria 21321, Egypt; saied1soliman@yahoo.com or saeed.soliman@alexu.edu.eg
[3] Department of Chemistry, University of Jyväskylä, P.O. Box 35, FI-40014 Jyvaskyla, Finland; matti.o.haukka@jyu.fi
[4] Department of Chemistry, College of Science, King Saud University, P.O. Box 2455, Riyadh 11451, Saudi Arabia
* Correspondence: ambarakat@ksu.edu.sa; Tel.: +966-11467-5901; Fax: +966-11467-5992

Citation: Altowyan, M.S.; Soliman, S.M.; Haukka, M.; Al-Shaalan, N.H.; Alkharboush, A.A.; Barakat, A. Synthesis of Unexpected Dimethyl 2-(4-Chlorophenyl)-2,3-dihydropyrrolo[2,1-*a*]isoquinoline-1,3-dicarboxylate via Hydrolysis/Cycloaddition/Elimination Cascades: Single Crystal X-ray and Chemical Structure Insights. *Crystals* **2022**, *12*, 6. https://doi.org/10.3390/cryst12010006

Academic Editor: Jesús Sanmartín-Matalobos

Received: 1 December 2021
Accepted: 16 December 2021
Published: 21 December 2021

Abstract: Hydrolysis/[3 + 2] cycloaddition/elimination cascades employed for the synthesis of unexpected tricyclic compound derived from isoquinoline. Reaction of ethylene derivative **1** with the isoquinoline ester iminium ion **2** in alkaline medium ($MeOH/NEt_3$) under reflux for 1 h resulted in the formation of the fused pyrrolo[2,1-*a*]isoquinoline derivative **3**. Its structure was elucidated by X-ray single crystal and other spectrophotometric tools. Hirshfeld calculations for **3** and its crystal structure analysis revealed the importance of the short O…H (19.1%) contacts and the relatively long H…C (17.1%), Cl…H (10.6%) and C…C (6.1%) interactions in the molecular packing. DFT calculations were used to compute the electronic and spectroscopic properties of the studied system. The studied compound has polar nature (3.5953 Debye). TD-DFT calculations assigned the shortest wavelength band (220 nm) to the HOMO−1→LUMO+2 (57%), HOMO−1→LUMO+4 (14%) mixed excitations. The calculated NMR chemical shifts correlated very well with the experimental data (R^2 = 0.93–0.94).

Keywords: pyrrolo[2,1-*a*]isoquinoline; azomethine ylide; [3 + 2] cycloaddition (32CA) reaction; stereoselective; DFT; Hirshfeld

1. Introduction

Quinoline and isoquinoline analogues are privileged structures which exploited for the synthesis of polyheterocycles for the applications in the therapeutic area [1–3]. Fused isoquinoline moiety with other heterocyles gained much attention in the drug discovery community, however many efficient synthetic protocols being reported in the last decade [4–8]. Pyrrolo[2,1-*a*]isoquinoline is a core structure in many natural products with pharmaceutical targets including human topoisomerase I inhibitors and anti-HIV-1 activities as lamellarins [9–11], and others such as trollines, crispines, and oleraceins [1]. Indeed, this framework remarks as a skeleton for many synthesized molecules as important, interesting and attractive goal in organic synthesis.

[3 + 2] Cycloaddition reaction via azomethine ylide is one of the most straightforward, powerful, and efficient reactions that offered the construction of fused tricyclic compound based on pyrrolo[2,1-*a*]isoquinoline [12]. Many examples described in the literature for the synthesis of pyrrolo[2,1-*a*]isoquinolines using metal mediated syntheses such as

silver-catalyzed cycloisomerization/dipolar cycloaddition reported by Porco Jr. et al. [13]. Cascade oxidation/cycloaddition/aromatization catalyzed by copper was described by Wang and co-workers [14]. In addition, a very elegant example disclosed by Xiao in which $[Ru(bpy)_3]^{3+}$ catalyzed the oxidation/cycloaddition/aromatization cascade reactions [15]. Another elegant protocol is the Pd-catalyzed stereoselective four multicomponent synthesis of pyrrolidinyl-,pyrazolidinyl-, and isoxazolidinyl isoquinolines described by Grigg, R. et al. [16]. Among the reported procedures for the synthesis of pyrrolo[2,1-*a*]isoquinolines was to use the alkaline medium [17] or electrochemical synthesis [18] to generate the azomethine ylide as integral part of the dipolar [3 + 2] cycloaddition reaction.

The application of fused heterocyclic system based on imidazo[2,1-*b*]thiazole skeleton covers a vast therapeutic area as antimicrobial, anti-inflammatory, diuretic agents and human constitutive androstane receptor (CAR) agonist [19–21]. In this context, and in continuation of our interest to construct new heterocyclic systems by [3 + 2] cycloaddition (32CA) reaction [22–30], we employed the imidazo[2,1-*b*] thiazole based chalcone as a dipolarphile for the [3 + 2] cycloaddition (32CA) reaction to construct a new compound derived from pyrrolo[2,1-*a*]isoquinoline (**3**). Molecular insights including X-ray single crystal structure combined with Hirshfeld surface analysis of **3** were presented. In addition, DFT calculations were performed in order to compute the NMR chemical shifts and simulate the UV-Vis electronic spectra.

2. Materials and Methods

The synthesis of imidazo[2,1-*b*]thiazole derivative as a dipolarphile **1** and the monoquaternary salt **2** followed by the reported procedure in literature [31,32].

2.1. Synthesis of Dimethyl 2-(4-Chlorophenyl)-2,3-dihydropyrrolo[2,1-a]isoquinoline-1,3-dicarboxylate **3**

The monoquaternary salt **2** (1 mmol, 1 eq., 296 mg) and ethylene derivative **1** (1.0 mmol, 1.0 eq. 464 mg) were dissolved in MeOH (10 mL). Then, NEt_3 (1 mmol, 1 eq., 0.14 mL) was partially added under magnetic stirring, subsequently the reaction mixture was refluxed for 1 h which the progress of the reaction monitored by TLC (*n*Hexane–EtOAc (3:1). Evaporation the solvent and the crude product was purified by column chromatography on silica gel, eluting with petrol. ether–EtOAc (3:1), to give ester **3** (347 mg, 88%) as pale-yellow needles.

^{1}H NMR (400 MHz, $CDCl_3$) δ 9.85 (d, *J* = 8.4 Hz, 1H), 9.35 (d, *J* = 7.4 Hz, 1H), 8.63–8.56 (m, 1H), 7.75–7.68 (m, 1H), 7.56 (s, 2H), 7.15 (s, 1H), 6.69 (d, *J* = 6.6 Hz, 2H), 6.28 (d, *J* = 7.3 Hz, 1H), 4.56 (d, *J* = 3.0 Hz, 1H), 4.42 (d, *J* = 3.3 Hz, 1H), 3.83 (s, 2H), 3.53 (s, 3H). ^{13}C NMR (126 MHz, $CDCl_3$) δ 170.72, 166.06, 151.71, 143.31, 136.13, 132.82, 132.20, 131.46, 129.61, 128.99, 128.29, 126.68, 126.16, 123.76, 107.82, 95.40, 71.24, 53.30, 50.73, 50.53; IR (KBr, cm^{-1}): 3428, 2948, 2870, 1710, 1651, 1510, 107; Chemical formula: $C_{22}H_{18}ClNO_4$.

2.2. X-ray Single Crystal Measurements of **3**

The technical experimental data for the synthesized compound **3** and the software [33–36] employed for data processing was amended in the Supplementary Materials. The crystallographic details are summarized in Table 1.

Table 1. Crystal data and structure refinement for **3**.

Contact	3
CCDC	2075387
empirical formula	$C_{22}H_{18}ClNO_4$
fw	395.82
temp (K)	120(2) K
λ (Å)	0.71073 Å
cryst syst	Monoclinic
space group	$P2_1/c$

Table 1. *Cont.*

Contact	3
a (Å)	7.9337(3)
b (Å)	32.6514(8)
c (Å)	7.7034(3)
β (deg)	111.687(4)
V (Å^3)	1854.29(12) Å^3
Z	4
ρ_{calc} (mg/m^3)	1.418 mg/m^3
μ (Mo Kα) (mm^{-1})	0.236 mm^{-1}
No. reflns.	16,269
Unique reflns.	4791
GOOF (F^2)	1.027
R_{int}	0.0434
R_1 [a] ($I \geq 2\sigma$)	0.0477
wR_2 [b] ($I \geq 2\sigma$)	0.1017

[a] $R_1 = \Sigma \mid \mid F_o \mid - \mid F_c \mid \mid / \Sigma \mid F_o \mid$. [b] $wR_2 = [\Sigma[w(F_o^2 - F_c^2)^2] / \Sigma[w(F_o^2)^2]]^{1/2}$.

2.3. Computational Study

The protocols for the Hirshfeld surface analysis [37], DFT [38,39], NBO [40], self-consistent reaction filed (SCRF) calculations [41,42], as well as NMR computation [43] are provided in Supplementary Materials.

3. Results and Discussion

3.1. Chemistry

The unexpected tricyclic heterocyclic compound based on isoquinoline scaffold has been obtained from the starting material named (*Z*)-2-(4-chlorobenzylidene)-5,6-diphenylimidazo[2,1-*b*]thiazol-3(2*H*)-one **1** with the bromide salt of isoquinoline ester **2** in MeOH using basic medium and under reflux for 1 h. The generated azomethine ylide was involved in the reaction as intermediate which further move to [3 + 2] cycloaddition (32CA) reaction with the ethylene derivative **1** to afford the new constructed fused pyrrolidine ring. Initially, we expected to obtain either the two diastereisomers **5** or **6** but surprisingly the reaction afforded the tricyclic heterocyclic derivative **3**. A proposed mechanism for this unexpected reaction was presented in Scheme 1. First, the isoquinoline ester iminium ion in alkaline medium could be deprotonated to yield isoquinolinium ylide. The amidic bond of the dipolarphile could be hydrolyzed under the same condition to afford the corresponding dipolarphile-ester **7**. Subsequently, [3 + 2] cycloaddition (32CA) reaction between the isoquinolinium ylide and dipolarphile-ester affords dimethyl 2-(4-chlorophenyl)-2,3-dihydropyrrolo[2,1-*a*]isoquinoline- 1,3-dicarboxylate **3** in which the 4,5-diphenyl-1*H*-imidazole-2-thiol **4** serve as a good leaving group. To understand this reaction mechanism, a control experiment was carried out subsequently. The dipolarphile **1** was taken in alkaline medium (MeOH/NEt_3) under reflux for 2 h monitored by TLC (Ethyl acetate: *n*Hexane 20%), the reaction proceeded to give the corresponding ester **7** (Scheme 1). The chemical feature of the tricyclic heterocyclic compound **3** was assigned based on ^{1}H-NMR; ^{13}C-NMR; IR; and single crystal X-ray diffraction analysis.

3.2. Crystal Structure Description of **3**

Figure 1 presents the structure of **3** based on the X-ray diffraction analysis. Crystallographic details are depicted in Table 1 while the reported geometric parameters are listed in Table 2. The lattice parameters are a = 7.9337(3) Å, b = 32.6514(8) Å, c = 7.7034(3), β = 111.687(4)°. The molecule comprised three fused rings where the two rings **A** and **B** are perfectly planar to one another (Figure 1). In ring C, the N1C19C20C7 atoms are located in the same plane while C8 atom located out of this plane by 0.365 Å. Additionally, the N1C19C20C9 plane is slightly deviated from the mean plan passing through rings **A** and **B** by only 3.5° while deviated from the mean plane of ring **D** by 86.7° indicating that rings **C**

and **D** are nearly perpendicular to one another. The molecular conformation structure of this compound is stabilized by weak intramolecular C17-H17...O4 with donor-acceptor distances of 2.980(2) Å. For better clarity, this intramolecular hydrogen bonding interaction is presented as turquoise dotted color line in the left part of Figure 2 (left part).

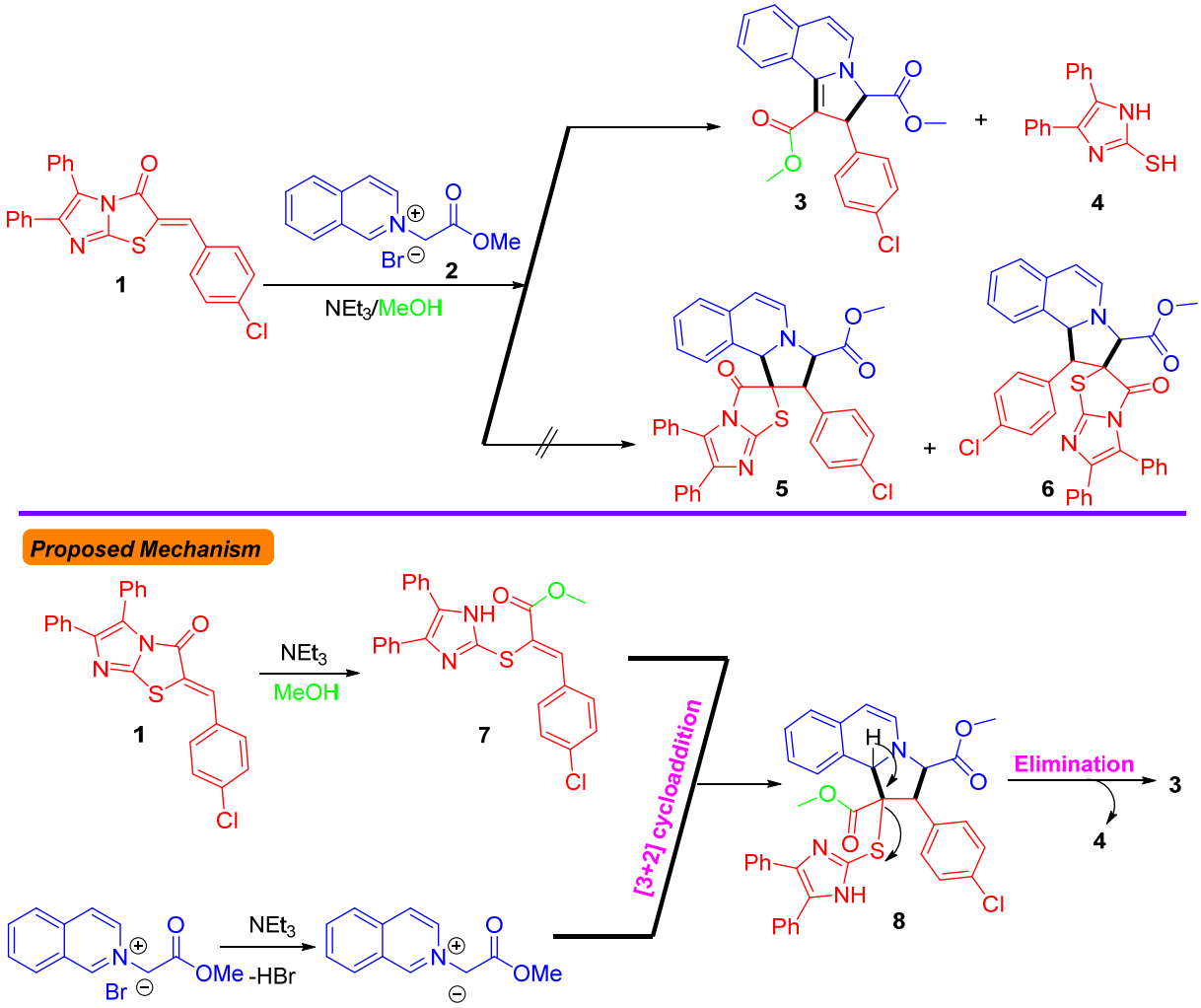

Scheme 1. Synthesis (**upper**) and proposed mechanism (**lower**) for the tricyclic heterocyclic compound based isoquinoline scaffold **3**.

The molecular packing of **3** is dominated by three hydrogen bonds shown as red dotted lines in Figure 2 (left part). The molecules are packed via non classical C-H...O interactions such as C8-H8...O4, C12-H12...O2, and C22-H22A...O1 contacts. The distances between the donor (D) and acceptor (A) are 3.245(2), 3.346(2) and 3.520(2) Å, respectively (Table 3). The molecular packing is shown in Figure 2 (right part).

Interestingly, the molecules are stacked to one another via aromatic π-π interactions of rings **A** with each other. This fact is clearly seen in the right part of Figure 2. The centroid-centroid distance between two stacked rings **A** is 3.882 Å and shortest C...C interaction of 3.521 and 3.559 Å for C11...C16 and C14...C18, respectively.

3.3. Analysis of Molecular Packing

The Hirshfeld surfaces of **3** is shown in Figure 3 while the whole set of intermolecular contacts contributing in the molecular packing are listed in Figure 4. In addition, summary of the shortest contacts is listed in Table 4. The molecules are mainly packed by short O...H (19.1%) contacts. These O...H contacts are shorter than the vdWs radii sum of the

interacting atoms with red regions in the d_{norm} maps (Figure 5). The O2...H12 (2.343 Å), O4...H8 (2.332 Å) and O1...H22A (2.499 Å) are the shortest C-H...O interactions. In addition, relatively long H...C (17.1%), Cl...H (10.6%) and C...C (6.1%) interactions are also dominant in the crystal packing (Figure 4). The H...H contacts are the most dominant with contact percentage of 44.8% from the whole fingerprint area. The absence of red/blue triangles in shape index and large green flat area in curvedness revealed the absence of significant π-π stacking interactions.

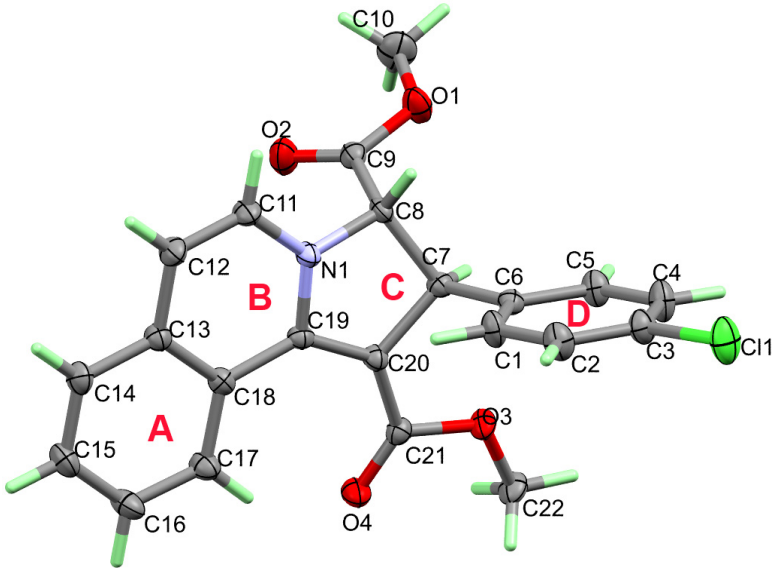

Figure 1. X-ray structure of **3**.

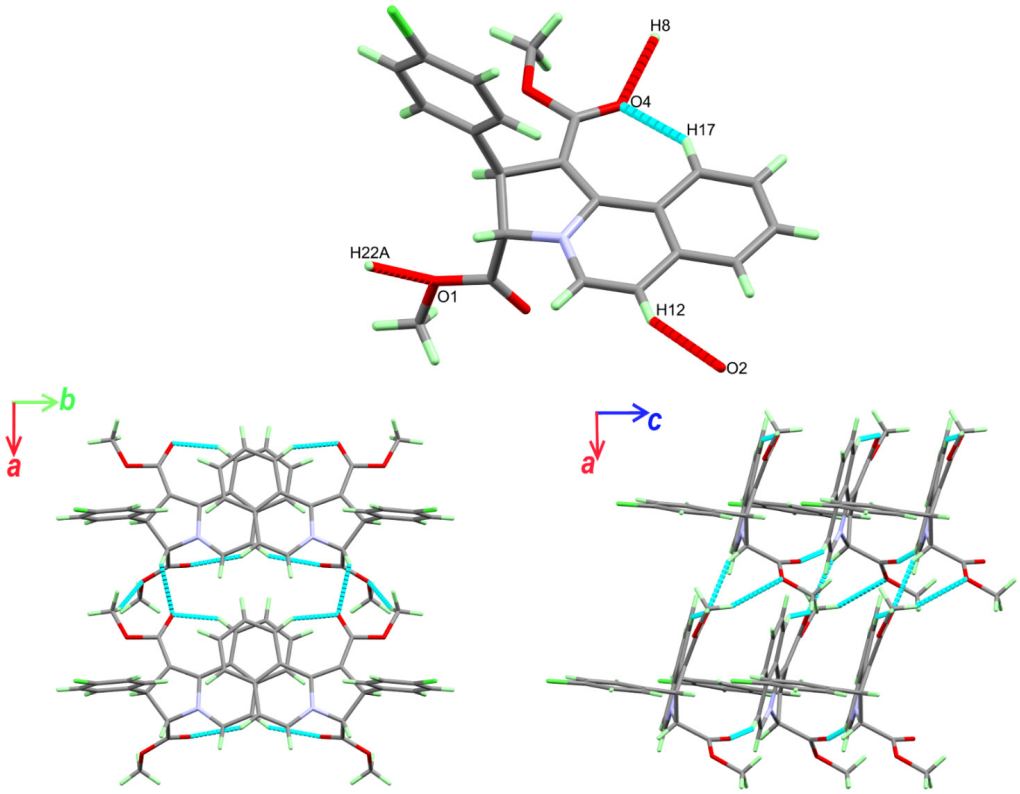

Figure 2. Hydrogen bonds in **3**.

Table 2. Bond lengths (Å) and angles (°) for **3**.

Bond	Length/Å	Bond	Length/Å
Cl1-C3	1.7425(19)	C6-C7	1.521(2)
O1-C9	1.338(2)	C7-C20	1.532(2)
O1-C10	1.455(2)	C7-C8	1.548(2)
O2-C9	1.194(2)	C8-C9	1.522(3)
O3-C21	1.370(2)	C11-C12	1.336(2)
O3-C22	1.436(2)	C12-C13	1.436(2)
O4-C21	1.223(2)	C13-C14	1.408(2)
N1-C11	1.376(2)	C13-C18	1.419(2)
N1-C19	1.382(2)	C14-C15	1.373(2)
N1-C8	1.457(2)	C15-C16	1.398(3)
C1-C2	1.388(3)	C16-C17	1.377(2)
C1-C6	1.389(2)	C17-C18	1.408(2)
C2-C3	1.385(3)	C18-C19	1.459(2)
C3-C4	1.379(3)	C19-C20	1.393(2)
C4-C5	1.392(3)	C20-C21	1.440(2)
Bonds	**Angle/′′**	**Bonds**	**Angle/′′**
C9-O1-C10	114.88(15)	O1-C9-C8	110.34(14)
C21-O3-C22	115.83(13)	C12-C11-N1	120.44(15)
C11-N1-C19	125.37(14)	C11-C12-C13	119.38(16)
C11-N1-C8	122.19(14)	C14-C13-C18	119.63(15)
C19-N1-C8	111.59(13)	C14-C13-C12	119.95(15)
C2-C1-C6	121.37(16)	C18-C13-C12	120.42(15)
C3-C2-C1	118.70(18)	C15-C14-C13	120.59(16)
C4-C3-C2	121.40(18)	C14-C15-C16	119.95(16)
C4-C3-Cl1	118.83(14)	C17-C16-C15	120.69(16)
C2-C3-Cl1	119.77(15)	C16-C17-C18	120.64(17)
C3-C4-C5	118.86 (17)	C17-C18-C13	118.48(15)
C6-C5-C4	121.23(17)	C17-C18-C19	122.55(15)
C5-C6-C1	118.43(16)	C13-C18-C19	118.97(14)
C5-C6-C7	119.92(16)	N1-C19-C20	109.02(14)
C1-C6-C7	121.62(15)	N1-C19-C18	115.39(14)
C6-C7-C20	114.86(14)	C20-C19-C18	135.58(15)
C6-C7-C8	111.81(13)	C19-C20-C21	131.92(15)
C20-C7-C8	101.56(13)	C19-C20-C7	109.13(13)
N1-C8-C9	109.27(14)	C21-C20-C7	118.95(14)
N1-C8-C7	103.02(13)	O4-C21-O3	120.31(14)
C9-C8-C7	111.47(14)	O4-C21-C20	130.41(16)
O2-C9-O1	124.11(18)	O3-C21-C20	109.25(14)
O2-C9-C8	125.55(16)		

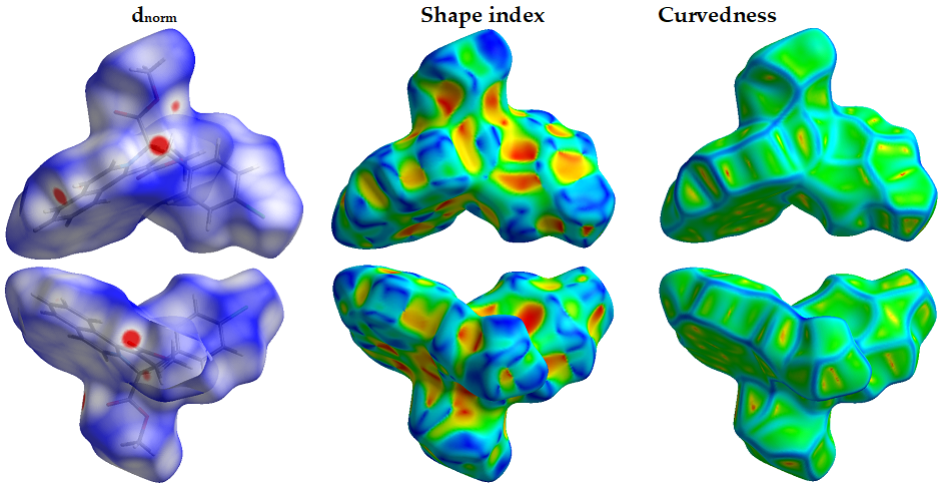

Figure 3. Hirshfeld surfaces of **3**.

Table 3. Hydrogen bond parameters (Å and °) for **3**.

D-H...A	D-H	H...A	D...A	D-H...A
C8-H8...O4 [1]	1.00	2.40	3.245(2)	142
C12-H12...O2 [2]	0.95	2.46	3.346(2)	155
C17-H17...O4	0.95	2.14	2.980(2)	147
C22-H22A...O1 [3]	0.98	2.59	3.520(2)	158

Symm. Code. [1] −1 + x,y,z; [2] x,1/2 − y,1/2 + z and [3] 1 + x,y,z.

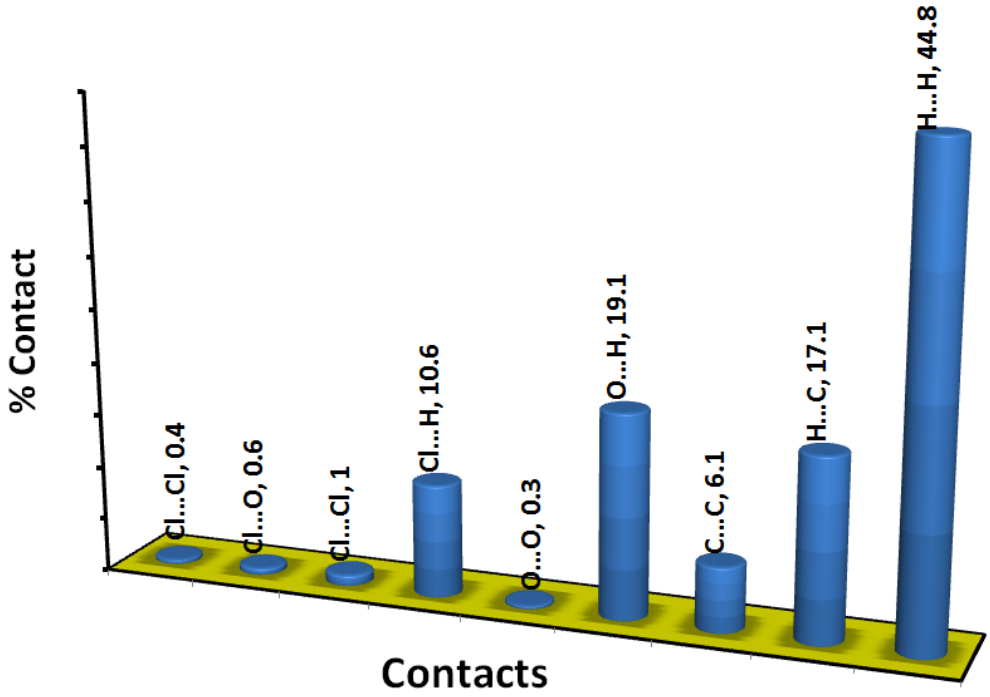

Figure 4. Intermolecular interactions in **3**.

Table 4. Shortest intermolecular interactions and their distances.

Contact	Distance	Contact	Distance
O2...H12 [1]	2.343	C17...C15 [4a]	3.644
O4...H8 [2]	2.332	C18...C14 [4a]	3.559
O1...H22A [3]	2.499	C21...H10C [5a]	2.879

[1] x,1/2 − y,1/2 + z; [2] −1 + x,y,z; [3] 1 + x,y,z; [4] x,1/2 − y, −1/2 + z; [5] 1 + x,y,1 + z [a] longer distances than the vdWs radii sum.

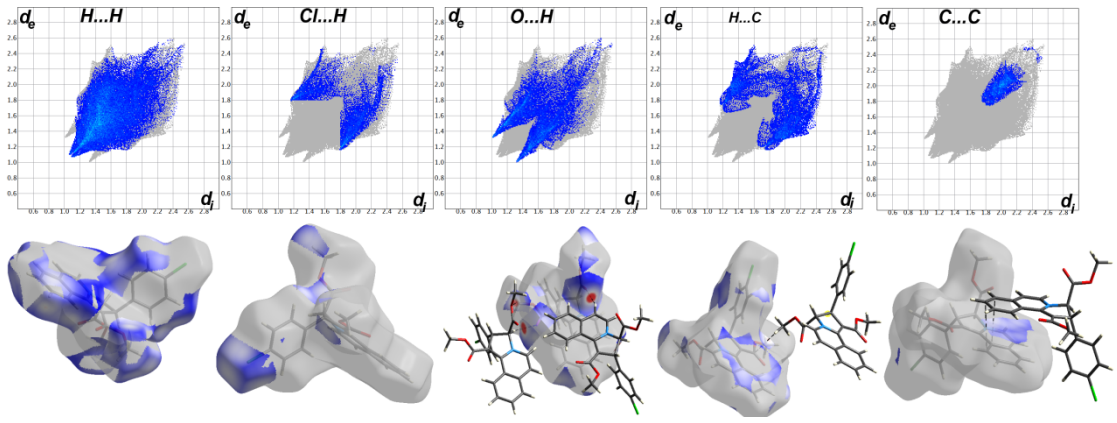

Figure 5. Decomposed fingerprint plots and d_{norm} surfaces in **3**.

3.4. DFT Studies

The structure of **3** was optimized and the resulting optimized geometry is compared with the experimental one (Figure 6). There is good matching between the calculated and experimental data (Table S1, Supplementary Materials). There are excellent straight-line correlations (R^2 = 0.9939–0.9599) between the calculated and experimental geometric parameters (Figure S4; Supplementary Materials). Crystal packing effects are main reason for the little differences between the computed and experimental structures.

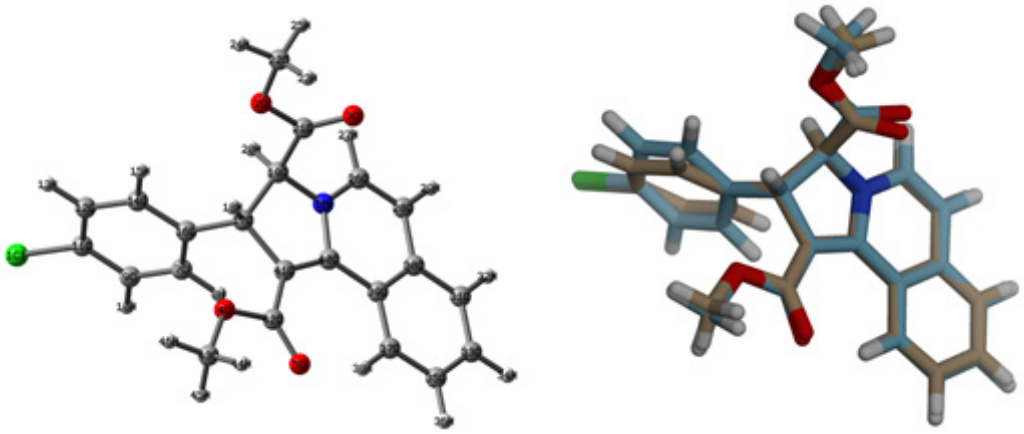

Figure 6. The calculated structure (**left**) and its overlay with experimental one, (**right**) for **3**.

The natural atomic charges were calculated and the results are depicted in Table S2 (Supplementary Materials). The results indicated the slight electronegative nature of chlorine atom (−0.0116 e). On the other hand, the nitrogen and oxygen atomic sites are electronegative where the two carbonyl oxygen atoms have higher charges than the two oxygen atoms bonded to the methyl groups. It is clear that the two oxygen atoms of the ester group attached to the sp^2 hybridized carbon atom have higher negative charges than the corresponding O-atoms of the ester group attached to the sp^3 hybridized carbon atom. The majority of carbon atoms have electronegative nature where the only exceptions are those C-atoms bonded either to N or O atoms. As a consequence of the presence of different charged regions in the studied molecule, the compound has polar nature (3.5953 Debye) and the dipole moment vector is presented in Figure 7.

In molecular electrostatic potential (MEP), there are intense red regions (highest e-density) close to the carbonyl oxygen atoms while the blue region (lowest e-density) closes to the CH proton of the sp^3 hybridized carbon atom bonded to the ester group (Figure 7). In the same figure, the HOMO and LUMO are located over the π-system of **3**. Hence, the HOMO→LUMO excitation is mainly π-π* transition. Based on the HOMO and LUMO energies, the reactivity indices such as ionization potential ($I = -E_{HOMO}$), electron affinity ($A = -E_{LUMO}$), chemical potential ($\mu = -(I + A)/2$), hardness ($\eta = (I-A)/2$) as well as electrophilicity index ($\omega = \mu^2/2\eta$) were calculated [44–50]. The calculated parameters are 5.0279, 1.3350, −3.1814, 3.6929 and 1.3704 eV, respectively.

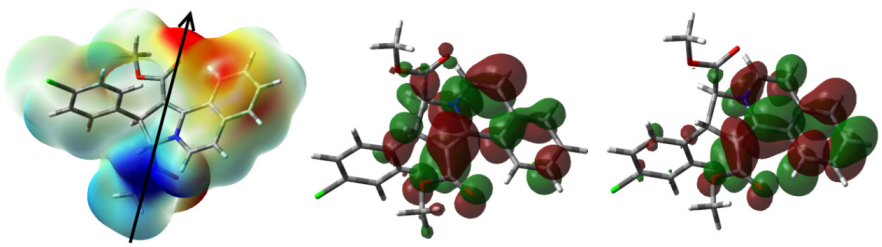

Figure 7. The MEP, HOMO and LUMO of **3**.

3.5. UV-Vis and NMR Spectra

The experimental UV-Vis spectra of the studied molecule were measured in different solvents as shown in the lower part of Figure 8. Obviously, the electronic spectra showed very little changes due to solvent effects. The UV-Vis spectra of the studied molecule exhibited several electronic transitions at 220, 272, 286, 298, 358, 397, 414 and 444 nm. Theoretically, the TD-DFT calculations predicted five electronic transitions calculated at 381.4 nm (f = 0.2416), 342.0 nm (f = 0.1837), 271.4 nm (f = 0.1269), 258.2 nm (f = 0.1157) and 220 nm (f = 0.1270) as shown in the upper part of Figure 8. The two bands calculated at 271.4 and 258.2 nm appeared in the theoretical TD-spectrum as one broad band mixed with a shoulder. The shortest wavelength band calculated at 220 nm is experimentally observed at the same wavelength and it was assigned to the H−1→L + 2 (57%) and H−1→L + 4 (14%) mixed excitations. Similarly, the electronic spectral bands observed experimentally at 272, 358 and 397 nm were predicted at 271.4, 342.0 and 381.4 nm, respectively. These spectral bands were assigned to H−1→LUMO (89%), HOMO→L + 1 (93%) and HOMO→LUMO (94%) excitations, respectively (Figure 9).

^{1}H and ^{13}C NMR chemical shifts (CSs) were calculated and compared with the experimental results (Table S3 (Supplementary Materials)) showing high correlation coefficients (R^2 = 0.93–0.94) which are close to 1 (Figure S5 Supplementary Materials).

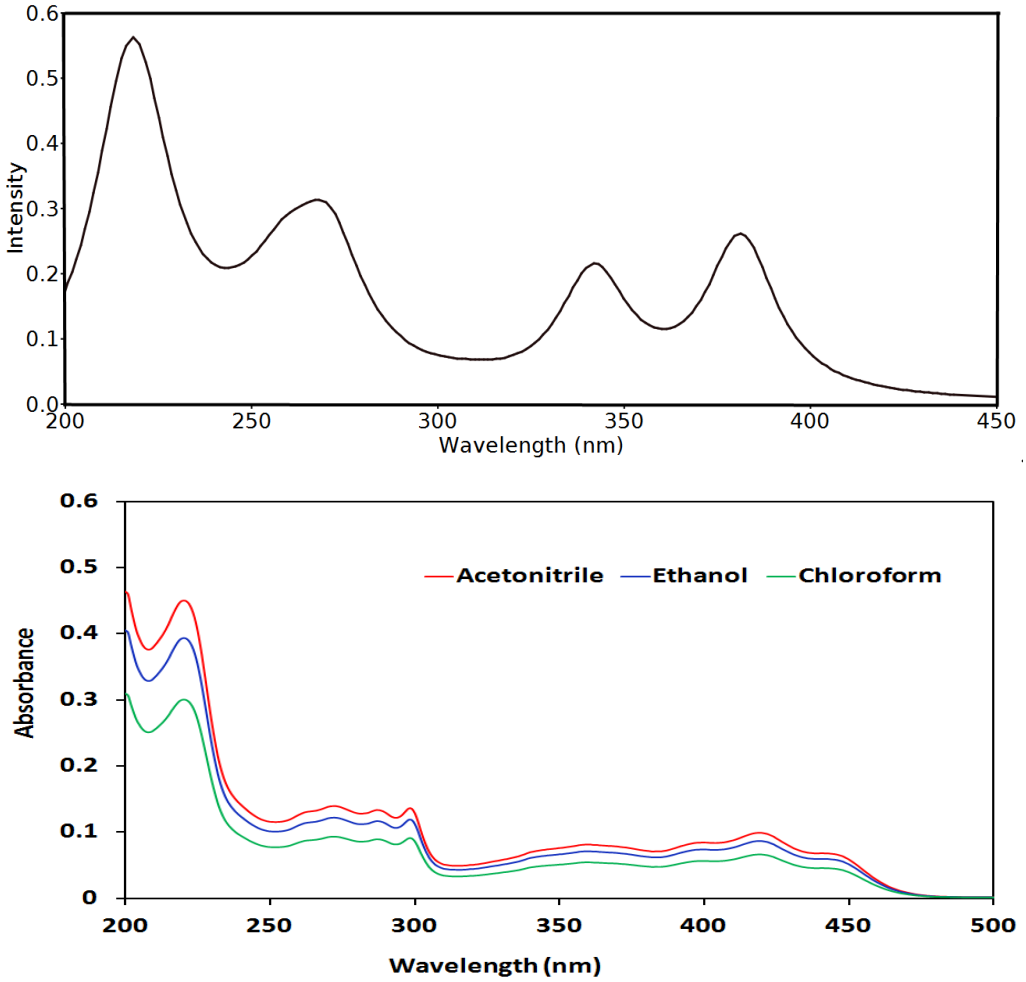

Figure 8. The calculated (**upper**) and experimental (**lower**) electronic spectra of **3**.

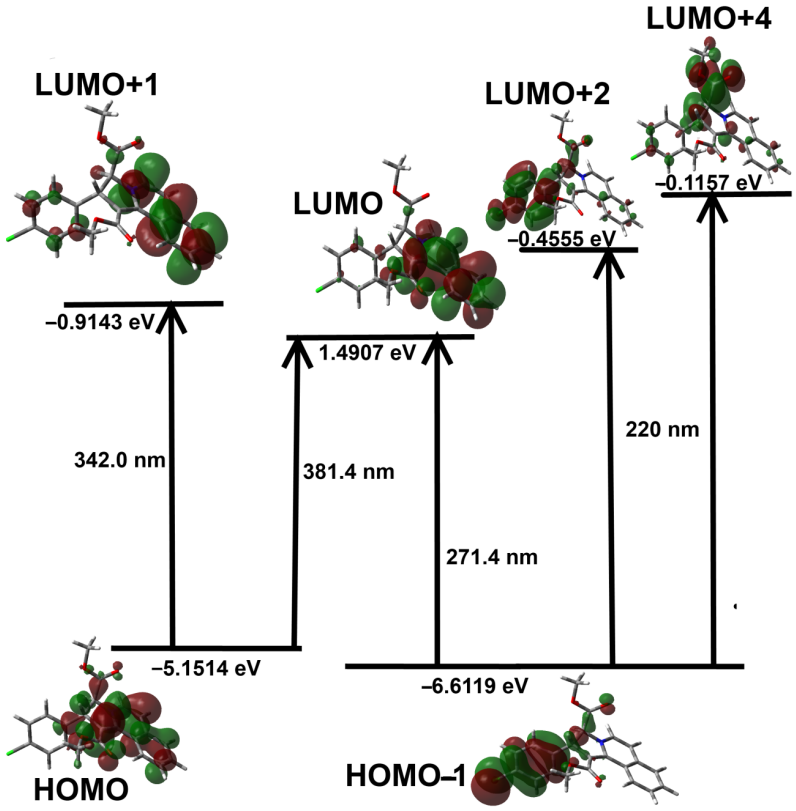

Figure 9. MOs included in the electronic absorption bands for the studied system.

4. Conclusions

In conclusion, we have been demonstrated the synthesis of a new pyrrolo[2,1-*a*]isoquinoline derivative via hydrolysis/[3 + 2] cycloaddition/elimination reactions incorporation cascades that proceed via azomthine ylide intermediate. Analysis of Hirshfeld surfaces indicated that the short O. . . H and the relatively long H. . . C, Cl. . . H and C. . . C interactions are the most significant while the H. . . H contacts are the most frequently occurring close interactions. DFT calculations were used to compute the electronic and spectroscopic properties of the studied system. The studied compound has polar nature (3.5953 Debye). The NMR chemical shifts and the UV-Vis spectral bands were calculated using GIAO and TD-DFT methods, respectively. This hypothesis could be useful and open insight to substrate scope with different substituents and examine the application of the new set of compounds against different targets.

Supplementary Materials: The following are available online at https://www.mdpi.com/article/10.3390/cryst12010006/s1, Figures S1–S3: ^{1}HNMR, ^{13}CNMR, and IR. Figure S4: Correlations between the optimized and experimental geometric parameters. Figure S5: ^{1}H and ^{13}C NMR correlations between the calculated and experimental data. Tables S1–S3: Computational investigations.

Author Contributions: Conceptualization, A.B.; methodology, M.S.A. and A.A.A.; software, S.M.S. and M.H.; validation, M.S.A., N.H.A.-S. and A.A.A.; formal analysis, M.S.A., N.H.A.-S., M.H. and A.A.A.; investigation, M.S.A.; resources, M.S.A. and A.B.; data curation, A.B. and S.M.S.; writing—original draft preparation, A.B. and S.M.S.; writing—review and editing, A.B. and S.M.S.; visualization, A.B., M.S.A. and N.H.A.-S.; supervision, A.B. and M.S.A.; project administration, A.A.A.; funding acquisition, M.S.A. All authors have read and agreed to the published version of the manuscript.

Funding: This work was funded by the Deanship of Scientific Research at Princess Nourah bint Abdulrahman University, through the Research Groups Program Grant no. (RGP-1443-0040).

Institutional Review Board Statement: Not applicable.

Informed Consent Statement: Not applicable.

Data Availability Statement: Not applicable.

Acknowledgments: This work was funded by the Deanship of Scientific Research at Princess Nourah bint Abdulrahman University, through the Research Groups Program Grant no. (RGP-1443 -0040).

Conflicts of Interest: The authors declare no conflict of interest.

References

1. Roesch, E.S. Isoquinolines. In *Privileged Scaffolds in Medicinal Chemistry: Design, Synthesis, Evaluation*; Brase, S., Ed.; RSC: Cambridge, UK, 2015; pp. 147–213.
2. Horton, D.A.; Bourne, G.T.; Smythe, M.L. The combinatorial synthesis of bicyclic privileged structures or privileged substructures. *Chem. Rev.* **2003**, *103*, 893–930. [CrossRef]
3. García-Castro, M.; Zimmermann, S.; Sankar, M.G.; Kumar, K. Scaffold diversity synthesis and its application in probe and drug discovery. *Angew. Chem. Int. Ed.* **2016**, *55*, 7586–7605. [CrossRef] [PubMed]
4. Sau, P.; Santra, S.K.; Rakshit, A.; Patel, B.K. *tert*-Butyl nitrite-mediated domino synthesis of isoxazolines and isoxazoles from terminal aryl alkenes and alkynes. *J. Org. Chem.* **2017**, *82*, 6358–6365. [CrossRef]
5. Gang, M.Y.; Liu, J.Q.; Wang, X.S. CuI-catalyzed Sonogashira reaction for the efficient synthesis of 1*H*-imidazo[2,1-*a*]isoquinoline derivatives. *Tetrahedron* **2017**, *73*, 4698–4705. [CrossRef]
6. Shi, R.G.; Sun, J.; Yan, C.G. Tandem double [3 + 2] cycloaddition reactions at both C-1 and C-3 atoms of N-cyanomethylisoquinolinium ylide. *ACS Omega* **2017**, *2*, 7820–7830. [CrossRef] [PubMed]
7. Leonardi, M.; Villacampa, M.; Menéndez, J.C. Mild and general synthesis of pyrrolo[2,1-*a*]isoquinolines and related polyheterocyclic frameworks from pyrrole precursors derived from a mechanochemical multicomponent reaction. *J. Org. Chem.* **2017**, *82*, 2570–2578. [CrossRef]
8. Al Matarneh, C.M.; Apostu, M.O.; Mangalagiu, I.I.; Danac, R. Reactions of ethylcyanoformate with cycloimmonium salts: A direct pathway to fused or substituted azaheterocycles. *Tetrahedron* **2016**, *72*, 4230–4238. [CrossRef]
9. Marco, E.; Laine, W.; Tardy, C.; Lansiaux, A.; Iwao, M.; Ishibashi, F.; Bailly, C.; Gago, F. Molecular determinants of topoisomerase I poisoning by Lamellarins: Comparison with Camptothecin and structure−activity relationships. *J. Med. Chem.* **2005**, *48*, 3796–3807. [CrossRef]
10. Reddy, M.V.R.; Rao, M.R.; Rhodes, D.; Hansen, M.S.T.; Rubins, K.; Bushman, F.D.; Venkateswarlu, Y.; Faulkner, D. Lamellarin α 20-sulfate, an inhibitor of HIV-1 integrase active against HIV-1 virus in cell culture. *J. Med. Chem.* **1999**, *42*, 1901–1907. [CrossRef]
11. Aubry, A.; Pan, X.-S.; Fisher, L.M.; Jarlier, V.; Cambau, E. Mycobacterium tuberculosis DNA gyrase: Interaction with quinolones and correlation with antimycobacterial drug activity. *Antimicrob. Agents Chemother.* **2004**, *48*, 1281–1288. [CrossRef]
12. Ploypradith, P.; Petchmanee, T.; Sahakitpichan, P.; Litvinas, N.D.; Ruchirawat, S. Total synthesis of natural and unnatural Lamellarins with saturated and unsaturated D-rings. *J. Org. Chem.* **2006**, *71*, 9440–9448. [CrossRef] [PubMed]
13. Su, S.; Porco, J.A., Jr. Synthesis of pyrrolo-isoquinolines related to the lamellarins using silver-catalyzed cycloisomerization/dipolar cycloaddition. *J. Am. Chem. Soc.* **2007**, *129*, 7744–7745. [CrossRef]
14. Yu, C.; Zhang, Y.; Zhang, S.; Li, H.; Wang, W. Cu (II) catalyzed oxidation-[3+ 2] cycloaddition-aromatization cascade: Efficient synthesis of pyrrolo [2,1-*a*] isoquinolines. *Chem. Commun.* **2011**, *47*, 1036–1038. [CrossRef]
15. Zou, Y.-Q.; Lu, L.-Q.; Fu, L.; Chang, N.-J.; Rong, J.; Chen, J.-R.; Xiao, W.-J. Visible-light-induced oxidation/[3 + 2] cycloaddition/oxidative aromatization sequence: A photocatalytic strategy to construct pyrrolo [2,1-a] isoquinolines. *Angew. Chem. Int. Ed.* **2011**, *50*, 7171–7175. [CrossRef]
16. Dondas, H.A.; Fishwick, C.W.; Gai, X.; Grigg, R.; Kilner, C.; Dumrongchai, N.; Kongkathip, B.; Kongkathip, N.; Polysuk, C.; Sridharan, V. Stereoselective palladium-catalyzed four-component cascade synthesis of pyrrolidinyl-, pyrazolidinyl-, and isoxazolidinyl isoquinolines. *Angew. Chem. Int. Ed.* **2005**, *44*, 7570–7574. [CrossRef]
17. Choi, A.; Morley, R.M.; Coldham, I. Synthesis of pyrrolo [1, 2-*a*] quinolines by formal 1, 3-dipolar cycloaddition reactions of quinolinium salts. *Beilstein J. Org. Chem.* **2019**, *15*, 1480–1484. [CrossRef] [PubMed]
18. Wang, Q.; Yuan, T.; Liu, Q.; Xu, Y.; Xie, G.; Lv, X.; Ding, S.; Wang, X.; Li, C. External oxidant-free oxidation/[3+ 2] cycloaddition/aromatization cascade: Electrochemical synthesis of polycyclic *N*-heterocycles. *Chem. Commun.* **2019**, *55*, 8398–8401. [CrossRef]
19. Andreani, A.; Granaiola, M.; Leoni, A.; Locatelli, A.; Morigi, R.; Rambaldi, M. Synthesis and antitubercular activity of imidazo [2, 1-*b*] thiazoles. *Eur. J. Med. Chem.* **2001**, *36*, 743–746. [CrossRef]
20. Maglich, J.M.; Parks, D.J.; Moore, L.B.; Collins, J.L.; Goodwin, B.; Billin, A.N.; Stoltz, C.A.; Kliewer, S.A.; Lambert, M.H.; Willson, T.M.; et al. Identification of a novel human constitutive androstane receptor (CAR) agonist and its use in the identification of CAR target genes. *J. Biol. Chem.* **2003**, *278*, 17277–17283. [CrossRef]
21. Hozien, Z.A.; Abd El-Wareth, A.S.; El-Sherief, H.A.; Mahmoud, A.M. An efficient route for synthesis of 5, 6-diphenylimidazo-[2,1-*b*] thiazoles as antibacterial agents. *J. Heterocycl. Chem.* **2000**, *37*, 943–949. [CrossRef]
22. Barakat, A.; Islam, M.S.; Ghawas, H.M.; Al-Majid, A.M.; El-Senduny, F.F.; Badria, F.A.; Elshaier, Y.A.; Ghabbour, H.A. Design and synthesis of new substituted spirooxindoles as potential inhibitors of the MDM2–p53 interaction. *Bioorg. Chem.* **2019**, *86*, 598–608. [CrossRef]

23. Altowyan, M.S.; Barakat, A.; Al-Majid, A.M.; Al-Ghulikah, H.A. Spiroindolone analogues bearing benzofuran moiety as a selective cyclooxygenase COX-1 with TNF-α and IL-6 inhibitors. *Saudi J. Biol. Sci.* **2020**, *27*, 1208–1216. [CrossRef]
24. Altowyan, M.S.; Barakat, A.; Al-Majid, A.M.; Al-Ghulikah, H. Spiroindolone analogues as potential hypoglycemic with dual inhibitory activity on α-amylase and α-glucosidase. *Molecules* **2019**, *24*, 2342. [CrossRef]
25. Islam, M.S.; Ghawas, H.M.; El-Senduny, F.F.; Al-Majid, A.M.; Elshaier, Y.A.; Badria, F.A.; Barakat, A. Synthesis of new thiazolo-pyrrolidine-(spirooxindole) tethered to 3-acylindole as anticancer agents. *Bioorg. Chem.* **2019**, *82*, 423–430. [CrossRef] [PubMed]
26. Barakat, A.; Islam, M.S.; Al Majid, A.M.; Ghawas, H.M.; El-Senduny, F.F.; Badria, F.A.; Elshaier, Y.A.M.M.; Ghabbour, H.A. Substituted spirooxindole derivatives as potent anticancer agents through inhibition of phosphodiesterase 1. *RSC Adv.* **2018**, *8*, 14335. [CrossRef]
27. Lotfy, G.; Aziz, Y.M.A.; Said, M.M.; El Sayed, H.; El Sayed, H.; Abu-Serie, M.M.; Teleb, M.; Dömling, A.; Barakat, A. Molecular hybridization design and synthesis of novel spirooxindole-based MDM2 inhibitors endowed with BCL2 signaling attenuation; a step towards the next generation p53 activators. *Bioorg. Chem.* **2021**, *117*, 105427. [CrossRef] [PubMed]
28. Barakat, A.; Soliman, S.M.; Al-majid, A.M.; Ali, M.; Islam, M.S.; Elshaier, Y.A.M.M.; Ghabbour, H.A. Regioselective synthesis of novel spiro-oxindole constructed with pyrrolidine/thioxothiazolidin-4-one derivatives: X-ray crystal structures, Hirshfeld surface analysis, DFT, docking and antimicrobial studies. *J. Mol. Struc.* **2018**, *1152*, 101–114. [CrossRef]
29. Aziz, Y.M.A.; Lotfy, G.; Said, M.M.; El Ashry, E.S.H.; El Tamany, E.S.H.; Soliman, S.M.; Abu-Serie, M.M.; Teleb, M.; Yousuf, S.; Dömling, A.; et al. Design, synthesis, chemical and biochemical insights into novel hybrid spirooxindole-based p53-MDM2 inhibitors with potential Bcl2 signaling attenuation. *Front. Chem.* **2021**, *9*, 735236. [CrossRef]
30. Al-Majid, A.M.; Soliman, S.M.; Haukka, M.; Ali, M.; Islam, M.S.; Shaik, M.R.; Barakat, A. Design, construction, and characterization of a new regioisomer and diastereomer material based on the spirooxindole scaffold incorporating a sulphone function. *Symmetry* **2020**, *12*, 1337. [CrossRef]
31. Mustafa, A.; Ali, M.I.; Abou-State, M.A.; Hammam, A.E.G. Reactions with 4, 5-disubstituted 2-mercaptoimidazoles and their derivatives. *J. Für Prakt. Chem.* **1972**, *314*, 785–792. [CrossRef]
32. Gherasim, C.; Airinei, A.; Tigoianu, R.; Craciun, A.M.; Danac, R.; Nicolescu, A.; Isac, D.L.; Mangalagiu, I.I. Synthesis and photophysical insights of new fused N-heterocyclic derivatives with isoquinoline skeleton. *J. Mol. Liq.* **2020**, *310*, 113196. [CrossRef]
33. Rikagu Oxford Diffraction. *CrysAlisPro*; Agilent Technologies Inc.: Yarnton, Oxfordshire, UK, 2018.
34. Sheldrick, G.M. ShelXT-Integrated space-group and crystal-structure determination. *Acta Cryst.* **2015**, *A71*, 3–8. [CrossRef]
35. Sheldrick, G.M. Crystal structure refinement with SHELXL. *Acta Cryst.* **2015**, *C71*, 3–8.
36. Hübschle, C.B.; Sheldrick, G.M.; Dittrich, B. ShelXle: A Qt graphical user interface for SHELXL. *J. Appl. Cryst.* **2011**, *44*, 1281–1284. [CrossRef]
37. Turner, M.J.; McKinnon, J.J.; Wolff, S.K.; Grimwood, D.J.; Spackman, P.R.; Jayatilaka, D.; Spackman, M.A. Crystal Explorer17. 2017, University of Western Australia: Perth, WA, Australia. Available online: http://hirshfeldsurface.net (accessed on 21 July 2017).
38. Frisch, M.J.; Trucks, G.W.; Schlegel, H.B.; Scuseria, G.E.; Robb, M.A.; Cheeseman, J.R.; Scalmani, G.; Barone, V.; Mennucci, B.; Petersson, G.A.; et al. *GAUSSIAN 09*; Revision A02; Gaussian Inc.: Wallingford, CT, USA, 2009.
39. *GaussView*; Version 4.1; Dennington, R., II; Keith, T.; Millam, J. (Eds.) Semichem Inc.: Shawnee Mission, KS, USA, 2007.
40. Reed, A.E.; Curtiss, L.A.; Weinhold, F. Intermolecular interactions from a natural bond orbital, donor-acceptor viewpoint. *Chem. Rev.* **1988**, *88*, 899–926. [CrossRef]
41. Marten, B.; Kim, K.; Cortis, C.; Friesner, R.A.; Murphy, R.B.; Ringnalda, M.N.; Sitkoff, D.; Honig, B. New model for calculation of solvation free energies: Correction of self-consistent reaction field continuum dielectric theory for short-range hydrogen-bonding effects. *J. Phys. Chem.* **1996**, *100*, 11775–11788. [CrossRef]
42. Tannor, D.J.; Marten, B.; Murphy, R.; Friesner, R.A.; Sitkoff, D.; Nicholls, A.; Ringnalda, M.; Goddard, W.A.; Honig, B. Accurate first principles calculation of molecular charge distributions and solvation energies from ab initio quantum mechanics and continuum dielectric theory. *J. Am. Chem. Soc.* **1994**, *116*, 11875–11882. [CrossRef]
43. Cheeseman, J.R.; Trucks, G.W.; Keith, T.A.; Frisch, M.J. A comparison of models for calculating nuclear magnetic resonance shielding tensors. *J. Chem. Phys.* **1996**, *104*, 5497–5509. [CrossRef]
44. Foresman, J.B.; Frisch, Æ. *Exploring Chemistry with Electronic Structure Methods*, 2nd ed.; Gaussian: Pittsburgh, PA, USA, 1996.
45. Chang, R. *Chemistry*, 7th ed.; McGraw-Hill: New York, NY, USA, 2001.
46. Kosar, B.; Albayrak, C. Spectroscopic investigations and quantum chemical computational study of (E)-4-methoxy-2-[(p-tolylimino) methyl] phenol. *Spectrochim. Acta* **2011**, *78*, 160–167. [CrossRef] [PubMed]
47. Koopmans, T.A. Ordering of wave functions and eigenenergies to the individual electrons of an atom. *Physica* **1933**, *1*, 104–113. [CrossRef]
48. Parr, R.G.; Yang, W. *Density-Functional Theory of Atoms and Molecules*; Oxford University Press: New York, NY, USA, 1989.
49. Parr, R.G.; Szentpaly, L.V.; Liu, S. Electrophilicity index. *J. Am. Chem. Soc.* **1999**, *121*, 1922–1924. [CrossRef]
50. Singh, R.N.; Kumar, A.; Tiwari, R.K.; Rawat, P.; Gupta, V.P. A combined experimental and quantum chemical (DFT and AIM) study on molecular structure, spectroscopic properties, NBO and multiple interaction analysis in a novel ethyl 4-[2-(carbamoyl) hydrazinylidene]-3, 5-dimethyl-1*H*-pyrrole-2-carboxylate and its dimer. *J. Mol. Strut.* **2013**, *1035*, 427–440. [CrossRef]